

Preparation and luminescence properties of $\text{Mg}_2\text{Sr}_{2-x}\text{TiO}_4: \text{Eu}^{3+}, \text{Gd}^{3+}$ red phosphors

You Li^{a,*}, HengJian Huang^a, LiMin Dong^b, Dan Li^b, WenHao Shi^a, JiaRong Yin^a

^aGuangxi Key Laboratory of Optical and Electronic Materials and Devices, Guilin University of Technology, Guilin 541004, China.

^bKey Laboratory of Engineering Dielectrics and Its Application, Ministry of Education, Harbin University of Science and Technology, Harbin, China

Titanate-based luminescent materials have a strong absorption capacity for blue and near-ultraviolet light. Here, a sol-gel method is used to prepare a high-efficiency red phosphor of magnesium titanate $\text{Mg}_2\text{Sr}_{2-x}\text{TiO}_4: \text{Eu}^{3+}, \text{Gd}^{3+}$ doped with rare-earth ions. The optimal doping concentrations of the activator rare earth ion Eu^{3+} and the sensitizer Gd^{3+} were investigated. Furthermore, the doping of a certain amount of Sr^{2+} and Na^+ effectively improves the luminescence properties of silicate luminescent materials. The luminescence spectrum shows that the luminescent material has red monochromaticity and the strongest red-light emission is 614nm, which can be used for WLED.

(Received November 16, 2022; Accepted February 17, 2023)

Keywords: Titanate, Red emitting phosphors, Luminescent property, Sol-gel technique

1. Introduction

To obtain high-quality white light obtained by phosphor-converted technology in LEDs, it is urgent to develop red luminescent materials with stable chemical properties and good luminescence performance, which can increase the color rendering index and improve the color temperature in LEDs [1-7]. One method to produce white light is to use blue GaN/InGaN light-emitting diode chips to coat yellow phosphor ($\text{Y}_3\text{Al}_5\text{O}_{12}:\text{Ce}^{3+}$, YAG: Ce), which can produce white light with high efficiency [8]. However, the white light-emitting diode generated by this method lacks red light-emitting elements and had been defective such to low color rendering index and high color temperature. Traditional red luminescent materials such as (Ca, Sr)S: Eu^{2+} had poor chemical stability, produce harmful gases when heated, and had poor light absorption efficiency (laser around 400nm cannot be effectively absorbed) [9]. Scholars [10-13] have done a lot of research to solve these problems, and they are committed to the development of cleaner red luminescent materials with better color rendering index and good color temperature. Saif et al. [14] used a sol-gel method to synthesize a new type of photoluminescence and non-toxic orange-red phosphor based on titanate, and toxicity experiments showed that its toxicity was very low. Dawei et al. [15] prepared a pure red phosphor $\text{K}_2\text{Ln}(\text{PO}_4)(\text{WO}_4): \text{Tb}^{3+}, \text{Eu}^{3+}$ (Ln=Y, Gd, and Lu) with high efficiency and adjustable emission. By adjusting the ratio of Eu^{3+} and Tb^{3+} , the emission color of $\text{K}_2\text{Ln}(\text{PO}_4)(\text{WO}_4): \text{Tb}^{3+}, \text{Eu}^{3+}$ can be tinted from green to pure red. The quantum efficiency of

* Corresponding author: liyou@glut.edu.cn

this phosphor excited at 394nm is as high as 76.45%.

The luminescent material doped with rare-earth ions has stable physical and chemical properties and has the advantages of different morphologies, different colors of light, and high color purity [16-18]. Airton et al. [19] reported the effect of Eu^{3+} doping concentration on the structural morphology and spectral properties of Ba_2SiO_4 and found that the emission intensity and quantum efficiency of the doped samples are the highest when the Eu^{3+} doping amount is 4% and 5%, respectively. Red phosphors doped with manganese in titanate had also been studied, but because of the low quantum efficiency of red phosphors doped with Mn^{4+} , its application in LEDs excited by blue chips was limited [20]. In addition, the emission of Mn^{2+} -doped red phosphors can be tinted from red to deep red, but this property had not been widely used [21]. Because of its stable physical and chemical properties, high vibration frequency, and low phonon energy, titanate have a good absorption capacity for blue and NUV light, it is very suitable for use as a luminescent substrate material [22]. Dan et al. [23] used a new sol-gel method to synthesize $\text{SrTiO}_3:\text{Pr}^{3+}$, Mg^{2+} , and $\text{SrTiO}_3:\text{Pr}^{3+}$, Al^{3+} phosphors based on titanate substrates and found that the addition of compensation ions increases the luminous efficiency of red phosphors ($\text{SrTiO}_3:\text{Pr}^{3+}$). Sanja et al. [24] studied the photoluminescence properties of $\text{Gd}_2\text{Ti}_2\text{O}_7$ nanoparticles synthesized under rare-earth doping (Sm^{3+} , Eu^{3+}), and found the strongest orange-red emission when doped with 2.5% Sm^{3+} .

In this paper, $\text{Mg}_2\text{Sr}_{2-x}\text{TiO}_4:\text{Eu}^{3+}$, Gd^{3+} red phosphors were synthesized by the sol-gel method, and the structure and luminescence properties of $\text{Mg}_2\text{Sr}_{2-x}\text{TiO}_4:\text{Eu}^{3+}$, Gd^{3+} red phosphors doped with rare-earth ions were discussed. The interaction of Eu^{3+} and Gd^{3+} occupying the magnesium titanate lattice, as well as the energy transfer and luminescence properties of Eu^{3+} and Gd^{3+} in the titanate red luminescent material are studied, and the luminous intensity of this luminescent material is improved by doping compensator ions. The interaction of Eu^{3+} and Gd^{3+} occupying the magnesium titanate lattice, as well as the energy transfer and luminescence properties of Eu^{3+} and Gd^{3+} in the titanate red luminescent material are studied. The result shows that $\text{Mg}_2\text{Sr}_{2-x}\text{TiO}_4:\text{Eu}^{3+}$, Gd^{3+} red phosphors can be used for LEDs excited by NUV and blue light chips.

2. Experiment

$\text{Mg}(\text{NO}_3)_2$, $\text{Eu}(\text{NO}_3)_3$, $\text{Gd}(\text{NO}_3)_3$, and $\text{C}_{16}\text{H}_{36}\text{O}_4\text{Ti}$ were the main medicines needed, $\text{C}_6\text{H}_8\text{O}_7$ was used as a complexing agent, $\text{HO}(\text{CH}_2\text{CH}_2\text{O})_n\text{H}$ was used as a dispersant, mixed and stirred in a water bath at 80°C for 1 hour, and aged. Then it becomes a precursor gel. Then it was heat-treated twice in a high-temperature electronic furnace, respectively 380°C , 0.5h; 600°C , 1h; placed in a high-temperature electronic furnace at 1150°C , 5h calcined to obtain $\text{Mg}_2\text{Sr}_{2-x}\text{TiO}_4:\text{Eu}^{3+}$, Gd^{3+} powder. The crystal structure of the titanate red luminescent material was determined by using the HT100 X-ray diffractometer of American Airt Technology Co., Ltd., the radiation source was $\text{CuK}\alpha$, and the scanning was in the range of 10° To 90° ; Observe the surface morphology of the powder; the emission lifetime measurement and excitation and emission spectra were performed on the RF-5301PC fluorescence spectrophotometer (Shimadzu, Japan).

3. Results and discussion

Figure 1 shows a typical XRD pattern of $\text{Mg}_2\text{Sr}_{2-x}\text{TiO}_4: \text{Eu}^{3+}, \text{Gd}^{3+}$ phosphor prepared by the sol-gel method, in which no obvious heterogeneous peaks appear for the crystalline form of magnesium orthotitanate. The measured XRD patterns were compared with the JCPDS standard card, and the PDF card numbered 25-1157 was in good agreement with the crystalline form of magnesium orthotitanate (Mg_2TiO_4). This indicates that the doped rare earth ions Eu^{3+} and Gd^{3+} successfully entered the Mg_2TiO_4 lattice and replaced Mg^{2+} as isomorphous substitutes; the doped Eu^{3+} and Dy^{3+} ions did not affect the lattice structure of magnesium orthotitanate; So the main body of the prepared luminescent material is Mg_2TiO_4 . The SEM image in the inset shows that the powder has uniform particles, clear grain interfaces, a particle size of about the particle size is about $0.5\sim 1\mu\text{m}$, and the surface of the particles is smooth and nearly hexahedral, with good dispersion.

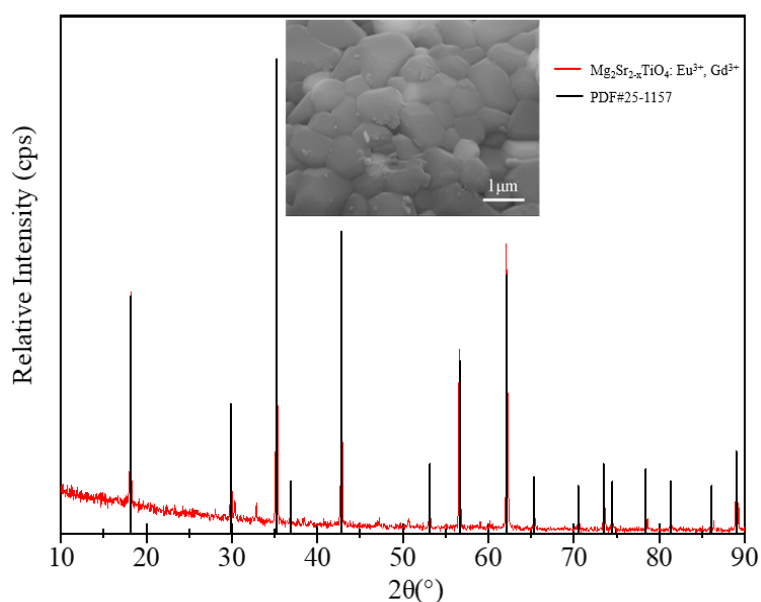


Fig. 1. XRD pattern of $\text{Mg}_2\text{Sr}_{2-x}\text{TiO}_4: \text{Eu}^{3+}, \text{Gd}^{3+}$ phosphor, the inset in Figure 1 is the SEM micrograph.

Fig. 2 gives the excitation and emission spectrogram of the $\text{Mg}_2\text{Sr}_{2-x}\text{TiO}_4: \text{Eu}^{3+}, \text{Gd}^{3+}$ phosphors. From Fig. 3, we observe that the excitation spectra of the phosphor are in the range of $340\sim 480\text{nm}$ and under the excitation of 394nm . The broad excitation bands appear in the short-wavelength range due to the charge transfer and absorption between O-Ti. In the long-wavelength range, the two highest emission peaks around 395nm and 465nm are ascribed to the Eu^{3+} electric dipole transition of ${}^7\text{F}_0\rightarrow{}^5\text{L}_6$, ${}^7\text{F}_0\rightarrow{}^5\text{D}_2$, respectively.

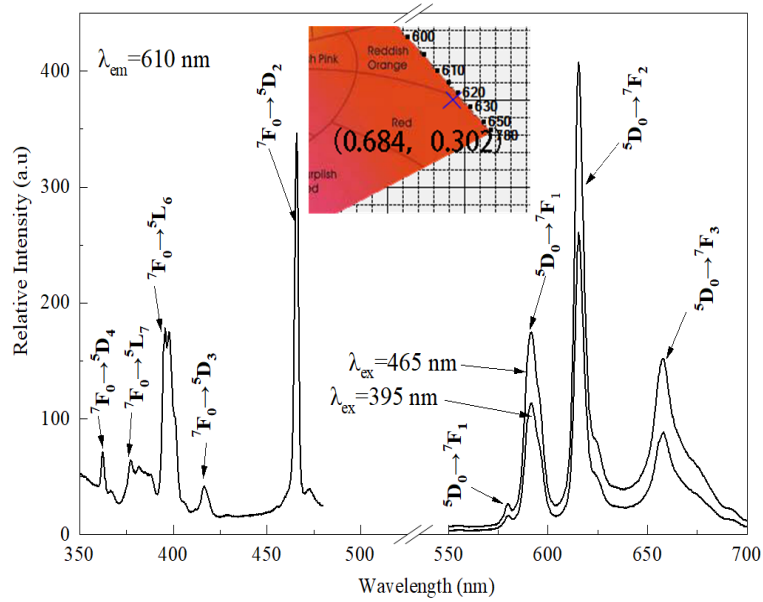


Fig. 2. Excitation and emission spectrogram of $\text{Mg}_2\text{Sr}_{2-x}\text{TiO}_4:\text{Eu}^{3+}, \text{Gd}^{3+}$ luminescent materials, the insert in Figure 2 represents CIE coordinates of partial emission spectra in $\lambda_{\text{ex}}=465\text{nm}$.

The excitation peaks of $\text{Mg}_2\text{Sr}_{2-x}\text{TiO}_4:\text{Eu}^{3+}, \text{Gd}^{3+}$ phosphors at 395nm and 465nm can correspond to the excitation wavelengths of near-ultraviolet and blue chips, respectively, which indicates that the WLEDs excited by NUV light and blue light both can be applied. The corresponding emission spectra under the 395nm and 465nm excitation shown in Fig. 2 display both have the same peak shape. Among these emission transitions of Eu^{3+} , ${}^5\text{D}_0 \rightarrow {}^7\text{F}_1$ (578nm, 591nm), ${}^5\text{D}_0 \rightarrow {}^7\text{F}_2$ (614nm), and ${}^5\text{D}_0 \rightarrow {}^7\text{F}_3$ (657nm), the peak at 614nm is the most intense ones, which indicates that the titanate red luminescent material has good monochromaticity. Furthermore, the emission peak intensity is stronger when $\lambda_{\text{ex}}=465\text{nm}$, the CIE chromaticity coordinates of phosphor are close to red emission (0.684, 0.302), that phosphor show better red color purity and color temperature is 267805 K, which is a good low color temperature red luminescent material. These results suggest that the luminescent material is more suitable for use in LEDs excited by blue light chips.

Fig. 3 depicts the emission spectra of the different doping concentrations of Eu^{3+} that are excited at 465 nm. From Fig. 3, the peak shape and emission peak position of $\text{Mg}_2\text{Sr}_{2-x}\text{TiO}_4$ doped with Eu^{3+} remain unchanged. Furthermore, the luminous intensity of $\text{Mg}_2\text{Sr}_{2-x}\text{TiO}_4:\text{Eu}^{3+}, \text{Gd}^{3+}$ is effectively improved with the increase of Eu^{3+} doping. Among the various concentration of Eu^{3+} , 2.5%mol shows the strongest absorption. When the concentration of Eu^{3+} is more than 2.5%, the emission intensity starts decreasing due to the activator ions being doped too much, and the energy enters the quenching site, which makes the matrix and the luminescent center produce non-radiative energy transfer, and the concentration quenching causes the luminous intensity to decrease. So, the best Eu^{3+} ions doping concentration is 2.0mol%.

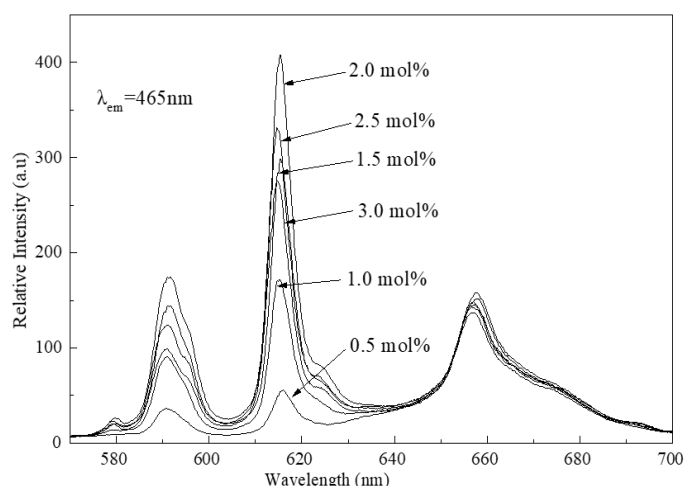


Fig. 3. Emission spectra (monitored at 465 nm) of the different doping concentrations of Eu^{3+} .

The emission spectra of $\text{Mg}_2\text{Sr}_{2-x}\text{TiO}_4:\text{Eu}^{3+}, \text{Gd}^{3+}$ phosphors doped with different ratio of $\text{Eu}^{3+}:\text{Gd}^{3+}$ under 465 nm is shown in Fig. 4. From Fig. 4, the presence of Gd^{3+} does not change the peak shape and emission peak position of $\text{Mg}_2\text{Sr}_{2-x}\text{TiO}_4$. It is observed that the luminescence intensity is the strongest when $\text{Mg}_2\text{Sr}_{2-x}\text{TiO}_4$ is doped with $\text{Eu}^{3+}:\text{Gd}^{3+}=1:1$, beyond which the luminescence intensity decreases. This result may be explained by the fact that the increase in the amount of Gd^{3+} promotes the energy transfer efficiency, the luminous intensity is improved, and the excessive amount of Gd^{3+} causes excessive energy to be consumed in the matrix through the quenching center, thereby reducing the luminous intensity. In consequence, the best molar ratio of Eu^{3+} to Gd^{3+} is 1:1.0.

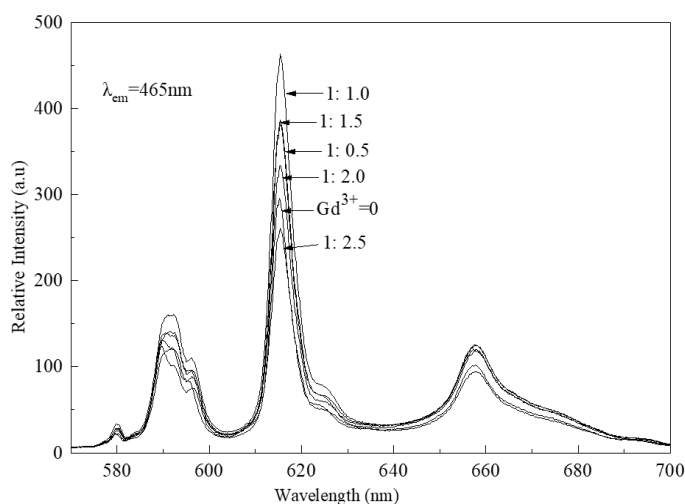


Fig. 4. Emission spectra of different ratios of $\text{Eu}^{3+}:\text{Gd}^{3+}$.

Fig. 5 shows the XRD patterns of $\text{Mg}_2\text{Sr}_{2-x}\text{TiO}_4$ doped with Ca^{2+} and Sr^{2+} . It is found that the diffraction peaks become sharper and the replacement effect of Sr^{2+} is the best when part of Mg^{2+} ions in $\text{Mg}_2\text{Sr}_{2-x}\text{TiO}_4$ are replaced by Ca^{2+} and Sr^{2+} ions, which indicates that the dopant Sr^{2+} ions can improve the atomic order and crystallinity of the luminescent material. The corresponding

SEM image (the inset of Fig. 5) can also be found that the luminescent materials replaced by other alkaline earth elements have a smaller particle size, and more uniform and regular particles, which shows that the doping of alkaline earth metals has an important effect on the surface morphology of the luminescent materials.

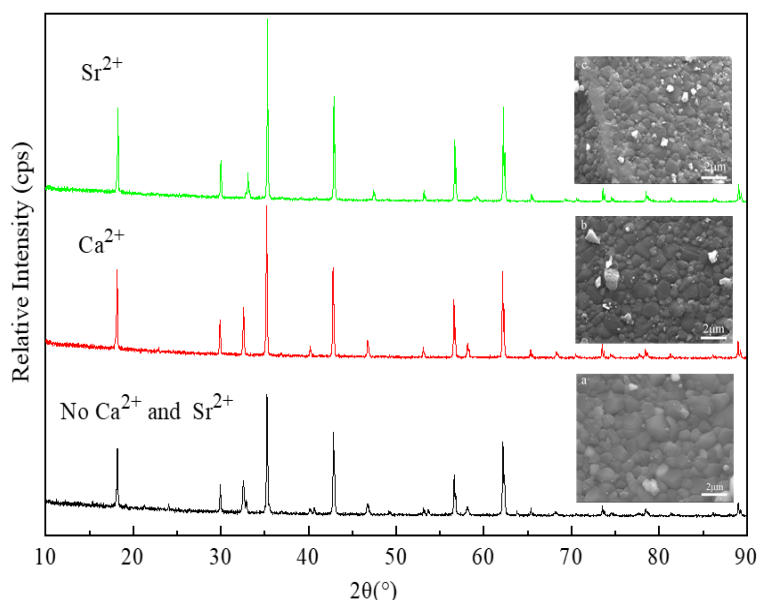


Fig. 5. XRD patterns of $Mg_2Sr_{2-x}TiO_4$ doped with Ca^{2+} and Sr^{2+} , the inset in Figure 5 is the corresponding SEM micrographs.

Figure 6 shows the emission spectra of the luminescent materials with Ca^{2+} , Sr^{2+} doping at 5 mol% with undoped Ca^{2+} , and Sr^{2+} ions under excitation at 465 nm. The peak positions of the emission spectra of the luminescent materials replaced with Ca^{2+} and Sr^{2+} changed, and the strongest emission peak was red-shifted from 610 nm to 614 nm without replacement, and a new emission peak appeared at 655 nm, and the luminescence intensity of the luminescent materials replaced with Sr^{2+} increased most significantly. Figure 6 inset for different Ca, Sr doping amount of luminous intensity comparison graph, with Ca^{2+} , Sr^{2+} doping increases, the luminous intensity of the luminous material is enhanced, doping Sr^{2+} effect is better. The main reason for this phenomenon is the doping of Ca^{2+} , and Sr^{2+} ions, the introduction of dopant ions destroys the original lattice layout of Mg_2TiO_4 , resulting in new defects within the structure, the larger the radius of the dopant ions so that the crystal tends to be more distorted, the lattice environment around the rare-earth ions Eu^{3+} further distorted, which is more conducive to the energy transfer of Eu^{3+} luminescence center, substantially improving the luminescent properties of light-emitting materials. At the same time when Eu enters the matrix lattice as a dopant ion, regardless of Eu^{2+} or Eu^{3+} , it can occupy the position of Sr^{2+} without destroying the crystal structure to achieve effective doping and thus improve the luminescence performance, which is the reason for the stronger emitted light from Sr^{2+} -replaced luminescent materials.

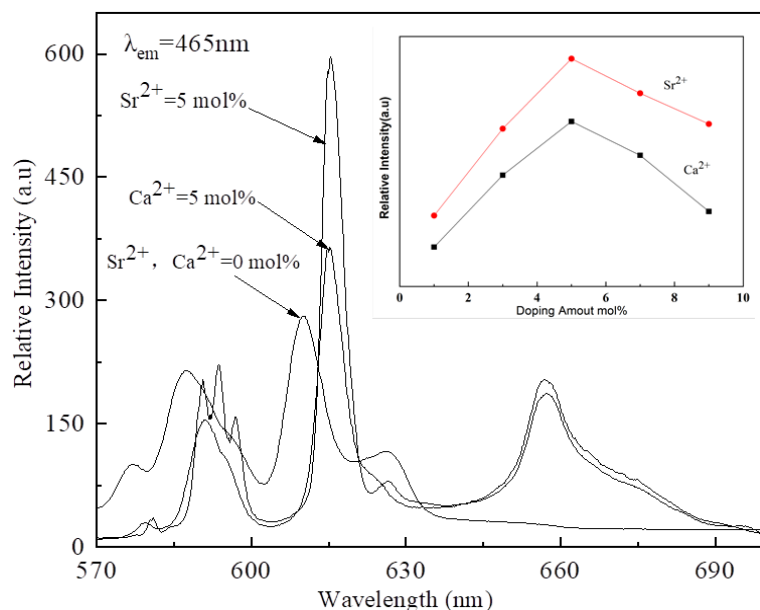


Fig. 6. The emission spectra of $\text{Mg}_2\text{TiO}_4:\text{Eu}^{3+}$, $\text{Mg}_2\text{Ca}_{2-x}\text{TiO}_4:\text{Eu}^{3+}$ ($\text{Ca}=5 \text{ mol}\%$), $\text{Mg}_2\text{Sr}_{2-x}\text{TiO}_4:\text{Eu}^{3+}$ ($\text{Sr}=5 \text{ mol}\%$), the inset shows the influence of the concentration on the emission intensity of $\text{Mg}_2\text{Sr}_{2-x}\text{TiO}_4:\text{Eu}^{3+}$, Gd^{3+} phosphor.

In $\text{Mg}_2\text{TiO}_4:\text{Eu}^{3+}$, one Eu^{3+} ion is expected to replace one Mg^{2+} ion. However, their charges are not equal, which makes it difficult to keep the charge balance in the host lattice and the luminous performance of the phosphor [18,25]. To solve the problem, the host has a doped charge compensation ion. Since Eu^{3+} replaces Mg^{2+} in the process of charge loss, the introduction of monovalent alkali metal ions can rebalance the charge of the host lattice, and enhance the luminescence, improve luminous characteristics. Both the diffraction peaks and half-peak width of the $\text{Mg}_2\text{Sr}_{2-x}\text{TiO}_4:\text{Eu}^{3+}$, Gd^{3+} phosphor have changed due to the incorporation of charge compensation ions can improve the atomic order degree and crystallinity of the phosphor to a certain extent, which can be seen from the XRD pattern of the luminescent material doped with Li^+ , Na^+ , and K^+ , etc. as a charge compensator (shown in Fig. 7). The inset in Fig. 7 shows the typical characteristic SEM image of the $\text{Mg}_2\text{Sr}_{2-x}\text{TiO}_4:\text{Eu}^{3+}$, Gd^{3+} phosphor. For all four samples, we found that the better surface morphology is the phosphor introduced with charge compensation ions, which has a crystallite size decrease, more uniform particle size, and better crystallinity, confirming that the best effect is the phosphor doped with Na^+ as the charge compensation ion.

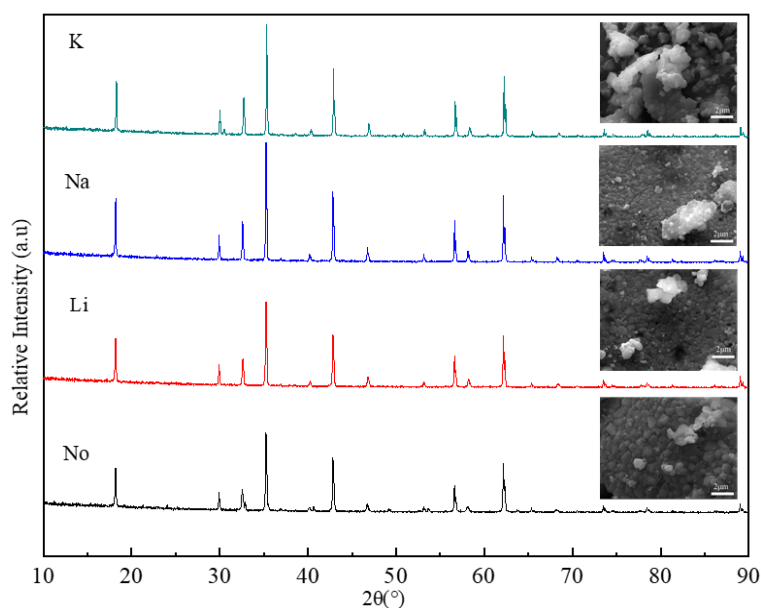


Fig. 7. XRD patterns of different alkali metal-doped, the inset in Figure 7 is the corresponding SEM micrographs.

Fig. 8 presents the emission spectra without and using Li^+ and $\text{Na}^+=1.5\% \text{mol}$, and $\text{K}^+=1.5\% \text{mol}$ as charge compensation ions. It is easy to notice that the phosphor with charge compensation ions has stronger luminous intensity than without charge compensation ions. Among Li^+ , Na^+ , and K^+ three charge compensation ions, the luminous effect of phosphor doped with Na^+ is the most significant. This result can be explained that the incorporation of alkali metal ions can compensate for the charge defects caused by the substitution of Eu^{3+} to replace Mg^{2+} , which makes the internal charge balance of the crystal lattice, which is beneficial to the improvement of luminescence performance. Benefit the Li^+ and Na^+ has a smaller ionic size, they can easily enter the lattice gap to generate cation vacancies, resulting in faster ion diffusion efficiency and enhanced charge compensation. The smaller size ions have a high correlation with the oxygen vacancies, which can effectively reduce the non-radiative transition caused by oxygen vacancies and improve the luminescence performance. In contrast, the larger ion K^+ cannot enter the lattice gap. Therefore, there is a certain compensation effect at a lower content, so the luminous performance improvement is not as significant as Na^+ [18,25]. The variation of luminous intensity after doped alkali metal as a charge compensator is shown in the inset of Fig. 8. As the amount of alkali metal-doped increases, the luminescence intensity of the luminescent material first increases and then decreases. The luminous intensity is the strongest when Na^+ is used as a charge compensator, and the first-rank doped concentration is 1.5 mol%.

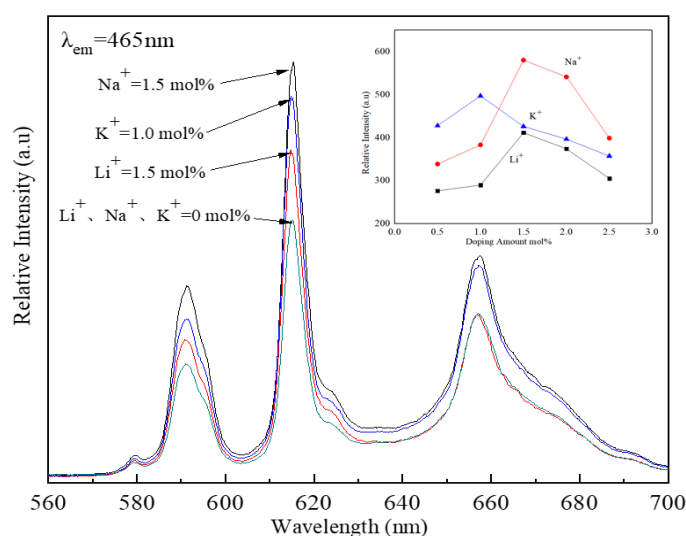


Fig. 8. Emission spectra of $\text{Mg}_2\text{Sr}_{2-x}\text{TiO}_4: \text{Eu}^{3+}, \text{Gd}^{3+}$ doped $\text{Li}^+, \text{Na}^+, \text{K}^+$, inset shows the variation of emission intensity of 465nm peaks as an influence of concentration of $\text{Li}^+, \text{Na}^+, \text{K}^+$.

4. Conclusions

Red emitting $\text{Mg}_2\text{Sr}_{2-x}\text{TiO}_4: \text{Eu}^{3+}, \text{Gd}^{3+}$ phosphor powder suitable for blue-chip excitation has been successfully prepared by the sol-gel method. The position of the main excitation peaks at 395 nm and 465 nm. The main emission peak is located at 597 nm, 614 nm, and 655 nm, which dramatically intense red emission at 614 nm. As we can see from the experimental consequences that the luminous intensity of the $\text{Mg}_2\text{Sr}_{2-x}\text{TiO}_4: \text{Eu}^{3+}, \text{Gd}^{3+}$ phosphor is the strongest, when the compensation ion concentration is $\text{Eu}^{3+}=2\% \text{mol}$, $\text{Eu}^{3+}: \text{Gd}^{3+}=1:1$, $\text{Sr}^{2+}=5\% \text{mol}$, $\text{Na}^+=1.5\% \text{mol}$, respectively. The incorporation of replacement elements results in a redshift of the emission peak. It is demonstrated that the phosphor replaced with Sr^{2+} emits stronger light because the Sr^{2+} ion radii are closer to Eu^{3+} and Eu^{2+} , which is more conducive to doping.

Acknowledgments

This work was supported by Project of Guangxi Base and Talents (AD19110086), the Supported Foundation of Guilin University of Technology (GUTQDJJ2018024), and the Open Foundation Guangxi Key Laboratory of Optical and Electronic Materials and Devices(22KF-13).

References

- [1] Y. Y. He, Y. Chen, R. Chen., Journal of Advances in Physical Chemistry 5(4), 83 (2016). (Convert English to Chinese)
- [2] L. Dolgov, J. Y. Hong, L. Zhou, et al., ACS Applied Materials & Interfaces 11(23), 21004 (2019); <https://doi.org/10.1021/acsami.9b05781>
- [3] X. H. Zhang, K. Yuan, L. L. Li, et al., Journal of Alloys and Compounds 762(25), 579 (2018);

<https://doi.org/10.1016/j.jallcom.2018.05.270>

[4] M. M. Medic, M. G. Brik, G. Drzic, et al., *The Journal of Physical Chemistry C* 119(1), 724 (2015); <https://doi.org/10.1021/jp5095646>

[5] M. Amela-Cortes, A. Garreau, S. Cordier, et al., *Journal of Materials Chemistry C* 2(8), 1545 (2014); <https://doi.org/10.1039/C3TC31309C>

[6] G. G. Li, J. Lin., *Chemical Society Reviews* 43(20), 7099 (2014);
<https://doi.org/10.1039/C4CS00109E>

[7] G. M. Cai, H.X. Liu, J. Zhang, et al., *Journal of Alloys and Compounds* 650, 494 (2015);
<https://doi.org/10.1016/j.jallcom.2015.08.026>

[8] Z. G. Xia, Q. L. Liu., *Progress in Materials Science* 84, 59 (2016);
<https://doi.org/10.1016/j.pmatsci.2016.09.007>

[9] X. Q. Liu, L. L. Liu, T. Zhan, et al., *New Chemical Materials* 44(5), 133 (2016) (Convert English to Chinese)

[10] R. Singh, J. Kaur, P. Bose, et al., *Journal of Materials Science: Materials in Electronics* 28, 13690 (2017); <https://doi.org/10.1007/s10854-017-7212-z>

[11] A. R. Zanatta, D. Scoca, F. Alvarez., *Journal of Alloys and Compounds* 780, 491 (2019);
<https://doi.org/10.1016/j.jallcom.2018.11.401>

[12] Z. Li, Y. F. Wang, J. Cao, et al., *Journal of Rare Earths* 34(2), 143 (2016);
[https://doi.org/10.1016/S1002-0721\(16\)60006-6](https://doi.org/10.1016/S1002-0721(16)60006-6)

[13] H. Chen, H. Lin, Q. M. Huang, et al., *Journal of Materials Chemistry C* 4, 2374 (2016).

[14] M. Saif, M. Shebl, A. Mbarek, et al., *Journal of Photochemistry and Photobiology A: Chemistry* 301, 1 (2015); <https://doi.org/10.1016/j.jphotochem.2014.12.014>

[15] D. W. Wen, J. J. Feng, J. H. Li, et al. *Journal of Materials Chemistry C* 3, 2107 (2014).

[16] G. Q. Fan, H. F. Lin, F. H. Shi, *Laser & Optoelectronics Progress* 49(3), 031602. 2012;
<https://doi.org/10.3788/LOP49.031602>

[17] V. A. Morozov, M. V. Raskina, B. I. Lazoryak, et al., *Chemistry of Materials* 26, 7124 (2014);
<https://doi.org/10.1021/cm503720s>

[18] A. K. V. Raj, P. P. Rao, T.S. Sreena, et al., *Physical Chemistry Chemical Physics* 19(30), 20110 (2017); <https://doi.org/10.1039/C7CP02741A>

[19] A. G. B. Jr, D. A. Ceccato, S. A. M. Lima, et al., *The Royal Society of Chemistry* 7, 53752 (2017); <https://doi.org/10.1039/C7RA10494D>

[20] H. M. Zhu, C.C. Lin, W. Q. Lou, et al., *Nature Communications* 5, 4312 (2014).

[21] Qiang Zhou, L. Dolgov, A. M. Srivastava, et al., *Journal of Materials Chemistry C* 6, 2652 (2018); <https://doi.org/10.1039/C8TC00251G>

[22] S. Y. Xu, T. Sun, L. L. Liu, et al., *Materials Reports* 28(03), 68 (2014). (Convert English to Chinese)

[23] Dan Guo, X. D. Zhang, J. G. Yun., *Advances in OptoElectronics* 10, 674 (2014);
<https://doi.org/10.1155/2014/674780>

[24] S. Culubrk, Z. Antic, M. Marinovic-Cincovic, et al., *Optical Materials* 37, 598 (2014).

[25] S. K. Shi, J. Gao, J. Zhou, et al., *Optical Materials* 30, 1616 (2008);
<https://doi.org/10.1016/j.optmat.2007.10.007>